

---

# Princeton Plasma Physics Laboratory

---

PPPL-

PPPL-



Prepared for the U.S. Department of Energy under Contract DE-AC02-09CH11466.

# Princeton Plasma Physics Laboratory

## Report Disclaimers

---

### Full Legal Disclaimer

This report was prepared as an account of work sponsored by an agency of the United States Government. Neither the United States Government nor any agency thereof, nor any of their employees, nor any of their contractors, subcontractors or their employees, makes any warranty, express or implied, or assumes any legal liability or responsibility for the accuracy, completeness, or any third party's use or the results of such use of any information, apparatus, product, or process disclosed, or represents that its use would not infringe privately owned rights. Reference herein to any specific commercial product, process, or service by trade name, trademark, manufacturer, or otherwise, does not necessarily constitute or imply its endorsement, recommendation, or favoring by the United States Government or any agency thereof or its contractors or subcontractors. The views and opinions of authors expressed herein do not necessarily state or reflect those of the United States Government or any agency thereof.

### Trademark Disclaimer

Reference herein to any specific commercial product, process, or service by trade name, trademark, manufacturer, or otherwise, does not necessarily constitute or imply its endorsement, recommendation, or favoring by the United States Government or any agency thereof or its contractors or subcontractors.

---

## PPPL Report Availability

### Princeton Plasma Physics Laboratory:

<http://www.pppl.gov/techreports.cfm>

### Office of Scientific and Technical Information (OSTI):

<http://www.osti.gov/bridge>

---

### Related Links:

[U.S. Department of Energy](#)

[Office of Scientific and Technical Information](#)

[Fusion Links](#)

# Electrostatic Detection of Stainless Steel Dust Particles for Fusion Applications

P. Landy,<sup>1</sup> C. H. Skinner,<sup>2</sup> and H. Schneider<sup>2</sup>

<sup>1</sup>*Department of Mechanical and Aerospace Engineering, Cornell University, Ithaca, New York, 14853, USA*

<sup>2</sup>*Princeton Plasma Physics Laboratory, Princeton, New Jersey 08543, USA*

(Received 4 February 2014; accepted 12 March 2014; published online XXXXX)

Dust accumulation inside next-step fusion devices poses a significant safety concern and dust diagnostics will be needed to assure safe operations. An electrostatic dust detection device has been successfully demonstrated in the National Spherical Torus Experiment (NSTX), Tore Supra and the Large Helical Device (LHD) and the detector's response to carbon particles was previously characterized in laboratory experiments. This paper presents laboratory results showing that detection of stainless steel particles at levels as low as several  $\mu\text{g}/\text{cm}^2$  is also possible.

Dust buildup from the erosion of plasma-facing components is a significant operational and safety concern for future magnetic fusion devices such as ITER<sup>1</sup>. Dust particles can be radioactive, chemically reactive, or toxic, posing safety issues in accident scenarios. Transport of dust into the plasma could affect plasma performance and potentially coat diagnostic first mirrors.

A vacuum-compatible remote dust detector is required for the management of dust. An electrostatic dust detector for carbon and lithium particles has been developed in laboratory experiments<sup>2,3,4</sup> and has been successfully applied to dust detection in the National Spherical Torus Experiment (NSTX)<sup>5</sup>, Tore Supra<sup>6</sup> and the Large Helical Device (LHD)<sup>7</sup>. The detector consists of a square grid of 25  $\mu\text{m}$  wide interlocking copper traces, separated by 25  $\mu\text{m}$  and biased to 50 V DC. Dust particles that impinge on the grid cause transient short circuits, creating voltage excursions across a resistor in a detection circuit. This waveform is filtered and quantified using counting electronics. The sensitivity for carbon particles with a count median diameter of 2.14  $\mu\text{m}$  was 0.15  $\text{ng}/\text{cm}^2/\text{count}$ , and for lithium particles of average diameter 44  $\mu\text{m}$  was 14.5  $\text{ng}/\text{cm}^2/\text{count}$ , both measured in vacuum<sup>4</sup>.

ITER will have tungsten and stainless steel plasma-facing surfaces and hence generate dust from these materials<sup>1</sup>. Initial laboratory trials showed that tungsten dust tended to damage the copper traces on the detector. A more rugged detector based on fine tungsten wires was developed<sup>8</sup> that was more durable than the copper grids used previously. However, sensitivity to tungsten was about 33 counts/mg, much lower than the copper grid. In this note we present the first results on the response of the copper grid dust detector to stainless steel particles and establish operating conditions that minimize any detector damage.

The experimental setup was similar to that described in Ref. 2. Dust was dropped in air on a 13 by 13 mm grid of fine interlocking copper traces on an Ultralam substrate. Trace widths and spacings were 25  $\mu\text{m}$ . Trials were performed with carbon and stainless steel particles. The carbon was prepared by scraping particles from a tile and sifting them through a 53  $\mu\text{m}$  aperture sieve<sup>9</sup>. Stainless steel particles labelled 'PF-5F' and 'PF-15F' were vendor supplied<sup>10</sup>. The dust particle size was measured by depositing dust on a glass slide and imaging it with a National Instruments DC5-163 digital optical microscope using a x10 objective and image pixel size of 0.5  $\mu\text{m}$ . Spatial calibration was performed with a 200  $\mu\text{m}$  calibration dot. The carbon dust mainly consisted of particles less than 10  $\mu\text{m}$  in diameter, but included agglomerates with diameters as large as 100  $\mu\text{m}$ . Particle agglomerates with diameters approaching 100  $\mu\text{m}$  were also observed for stainless steel particles. The dust images were analyzed with the ImageJ<sup>11</sup> size analysis program that treated the agglomerates as single particles. The particle size distribution function is plotted in Fig. 1 for both carbon particles and 'PF-5F' stainless steel particles. Using a spherical particle approximation<sup>9</sup>, the count median particle diameter (CMD) was 5.9  $\mu\text{m}$  for the carbon particles, 4.8  $\mu\text{m}$  for 'PF-5F' stainless steel particles, and 37.3  $\mu\text{m}$  for 'PF-15F' stainless steel particles.

Dust was distributed to the detector in air using the experimental setup shown in Figure 1 of Ref. 2. To remove large agglomerates of stainless steel particles, a sifter of 86  $\mu\text{m}$  aperture mesh size was used to pre-screen particles. A small spatula was used to load dust particles into a tray with a double or triple layer 86  $\mu\text{m}$  square mesh bottom. Multiple mesh layers helped to prevent dust from falling until needed. The mesh-bottomed tray was transported inside a larger, rectangular aluminum foil tray to help account for unintentional dust losses. The mesh

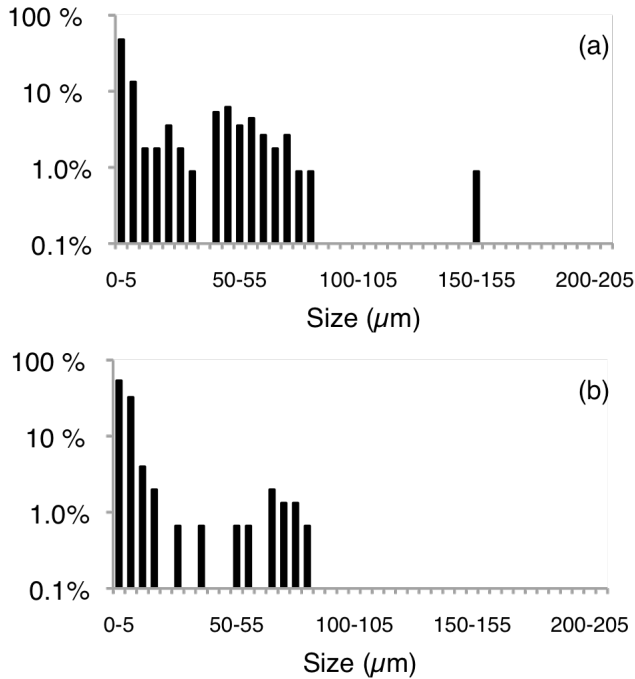


Fig. 1: Particle size distribution function for (a) carbon and (b) ‘PF-5F’ stainless steel dust particles. ‘Size’ is defined as the diameter of a spherical particle with equivalent projected area. The number of particles in each category is normalized to 100%.

tray was positioned above the detector in an open-bottomed cradle suspended from a 6” flange at the top of a cylindrical tube. The dust was released onto the grid through the mesh apertures of the containing tray by tapping the upper flange with a blunt object. The combined mass of the dust, mesh tray, and larger foil tray was measured before and after each trial using a Sartorius ME 5-F balance of precision 1 μg that was calibrated at least once a day. The value of each mass was recorded after the reading remained constant for 1 minute, and nitrile gloves and forceps were used to handle dust containers and equipment.

The mass of dust dropped on the detector grid during each trial was calculated from the mass lost by the dust tray. Some dust was lost during dust tray transport and this was accounted for by following the above procedure but without tapping the upper flange in order to not release dust onto the detector. The fraction of dropped dust incident on the grid was measured by replacing the detector with a small aluminum tray of the same dimensions as the grid area. An average of 18%, with standard deviation 12%, of 4.8 μm CMD stainless steel particles dropped through a triple mesh was incident on the grid area. Dust was not uniformly distributed on the mesh tray due to slight contours in the mesh material, and this may contribute to the standard deviation in this measurement. The areal mass density of dust particles incident on the grid was calculated for each trial by dividing the incident mass by the 1.6 cm<sup>2</sup> grid area.

Previous work<sup>12</sup> showed that heating by the current pulse caused up to 90% of carbon particles to be ejected from the grid or vaporized. High-speed videos<sup>13</sup> have shown tungsten particles striking the tungsten wire detector and then rapidly flying away or bouncing multiple times. The present trials used 4.8 μm CMD and 37.3 μm CMD stainless steel particles. The larger 37.3 μm particles were not effectively ejected from the grid and caused permanent short circuits, even at mass fluxes below 1 μg/cm<sup>2</sup>. The grid was tilted at 60° to aid ejection of particles from the grid, but no change in this behavior was observed. We note a possible particle removal solution was demonstrated in previous work that showed a He puffer was effective in removing residual carbon dust from the detector<sup>14</sup>.

The detector grid was biased to 50 ± 0.5 V using a Kepco ATE 325-0.8M power supply with a current limit set between 2 and 47 mA. The dust counting electronics are described in Ref. 2. Impinging dust particles created transient short circuits between the grid traces. These shorts created voltage spikes that were scaled, AC coupled and input to an Ortec 550A SCA (Single Channel Analyzer) and a Tektronix TDS5054B-NV digital phosphor oscilloscope. The SCA generated 5 V, 500 ns output pulses for input pulses that exceeded a lower threshold of 0.4 V but did not exceed an upper threshold of 10V. The SCA output pulses were counted using a Tennelec TC 534 counter and also monitored on the oscilloscope.

Trials conducted in air using the carbon dust showed a linear correlation between counts and areal mass density, and sensitivity that was consistent with previous

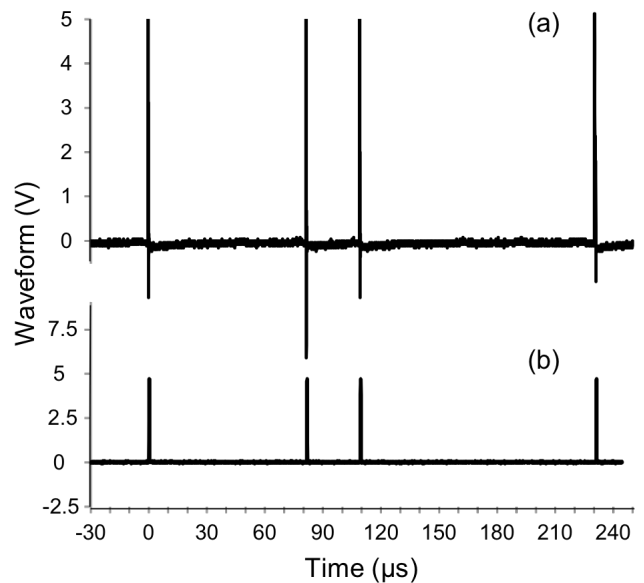


Fig. 2: (a) Example of a detector waveform generated by 4.8 μm CMD stainless steel particles and (b) the corresponding 5V SCA pulses.

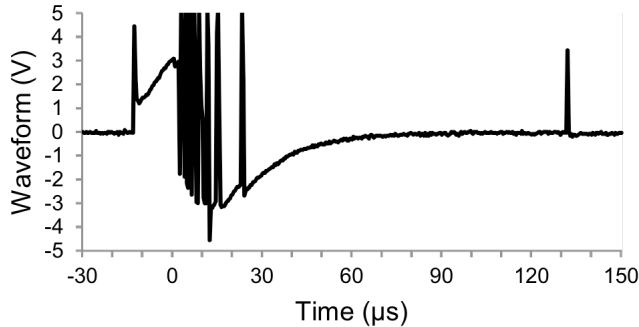


Fig. 3: Example of an oscillating waveform generated by the 4.8  $\mu\text{m}$  CMD stainless steel particles.

results<sup>3</sup>. Waveforms generated by 4.8  $\mu\text{m}$  CMD stainless steel particles in air were generally similar to those generated by carbon particles. Individual pulses usually lasted between 100 and 500 ns but had higher amplitudes, often exceeding the oscilloscope's limit of 5.17 V, presumably due to the lower resistivity of stainless steel. An example of a typical waveform generated by the detector and the corresponding SCA response is shown in Fig. 2. Past experience with tungsten particles<sup>8</sup> suggested that stainless steel particles might damage the copper traces. However, reducing the power supply current limit to 2 mA proved effective at preventing such damage.

Incidents where rapid pulse oscillation occurred were much more common for stainless steel particles, and negative amplitudes were much larger, often exceeding the lower limit of -5.17 V. These events were observed in the detector waveform in about one third of the trials with 4.8  $\mu\text{m}$  CMD stainless steel dust (see Fig. 3). It is possible that these were caused by dust agglomerates breaking apart upon contact with the grid and the resulting particles producing bursts of pulses. Carbon particles, which did not visibly clump together, rarely produced oscillating behavior, supporting the hypothesis that agglomeration is a cause for the oscillations.

The results of trials with 4.8  $\mu\text{m}$  CMD stainless steel particles using a current limit of 2 mA are shown in Fig. 4. A linear fit to this data through the origin yielded a sensitivity of 4 counts/ $\mu\text{g}/\text{cm}^2$ . However, the correlation coefficient was close to zero, indicating that correlation between counts and areal mass density is poor. Sources of scatter include the mass lost in each trial during tray transport, estimated at 20  $\mu\text{g}$  with a standard deviation of 10  $\mu\text{g}$ , and the variability in the fraction of dust incident on the grid. The high count frequency during the oscillation events led to pulse pileup and further impeded a consistent correlation between counts and areal mass density. Future work with finely filtered and evenly distributed stainless steel dust should reduce the scatter observed for stainless steel counts vs. areal mass density.

In summary the copper grid electrostatic dust detector produced counts for mass fluxes of stainless steel particles in air as low as several micrograms/ $\text{cm}^2$ . Limiting the current from the power supply to 2 mA was successful in preventing grid damage. An estimate for the detector's

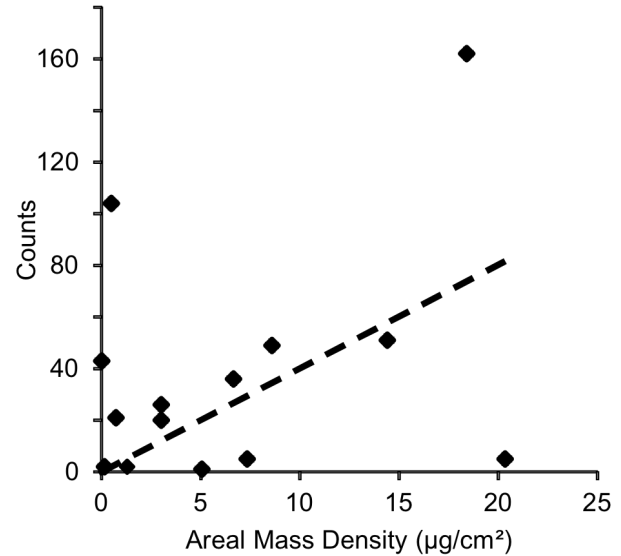


Fig. 4: Counts vs. areal mass density for 4.8  $\mu\text{m}$  CMD stainless steel particles.

sensitivity to 4.8  $\mu\text{m}$  median stainless steel particles is of order 4 counts/ $\mu\text{g}/\text{cm}^2$ , about 100 times lower than its sensitivity to carbon. The data to date shows low correlation between counts and stainless steel areal mass density. Oscillations in the waveform appear to be related to particle agglomeration.

The authors would like to thank T. Provost, T. Holoman, G. Smalley, and D. Labrie for their assistance with this research. This work was supported by a grant from the Department of Energy – SULI Program through contract no. DE-AC02-09CH11466.

<sup>1</sup>S. Rosanvallon, C. Grisolia, P. Andrew, S. Ciattaglia, P. Delaporte, D. Douai, D. Garnier, E. Gauthier, W. Gulden, S.H. Hong, S. Pitcher, L. Rodriguez, N. Taylor, A. Tesini, S. Vartanian, A. Vetry, M. Wykes, J. Nucl. Mater. 390-391 (2009) 57-60.

<sup>2</sup>D.P. Boyle, C.H. Skinner, A.L. Roquemore, J. Nucl. Mater. 390-391, 1086 (2009).

<sup>3</sup>C.H. Skinner, R. Hensley, A.L. Roquemore, J. Nucl. Mater. 376, 29-32 (2008).

<sup>4</sup>B. Rais, C.H. Skinner, A.L. Roquemore 'Absolute Calibration of an Electrostatic Dust Detector' Princeton Plasma Physics Lab Report PPPL-4537 (July 2010).

<sup>5</sup>C.H. Skinner, B. Rais, A.L. Roquemore, H.W. Kugel, R. Marsala, T. Provost, Rev. Sci. Instrum. 81, 10E102 (2010).

<sup>6</sup>H. Roche, A. Barbuti, J. Bucalossi, L. Ducobu, C. Grisolia, T. Loarer, B. Pegourie, S. Rosanvallon, P. Spuig, C. H. Skinner, S. Vartanian and B. Vincent, Phys. Scr. T145 014022 (2011).

<sup>7</sup>O. Motojima et al., Nucl. Fus. 43 1674 (2003).

<sup>8</sup>K. Hammond and C.H. Skinner 'Development of an Electrostatic Detector for Tungsten Dust' PPPL Technical Report 4970 (December 2013).

<sup>9</sup>C. Voinier, C. H. Skinner, A. L. Roquemore, J. Nucl. Mater. 346, 266-271 (2005).

<sup>10</sup>Epson Atmix Corporation, Aomori-ken, 039-1161 Japan

<sup>11</sup>ImageJ Image Processing and Analysis Software, NIH rsbweb.nih.gov/ij

<sup>12</sup>C.V. Parker, C.H. Skinner, A.L. Roquemore, J. Nucl. Mater. 363-365, 1461 (2007).

<sup>13</sup>D. Starkey personal communication, Aug 2012, unpublished.

<sup>14</sup>B. Rais, C. H. Skinner, and A. L. Roquemore Rev. Sci. Instrum. 82, 036102 (2011).

The Princeton Plasma Physics Laboratory is operated  
by Princeton University under contract  
with the U.S. Department of Energy.

Information Services  
Princeton Plasma Physics Laboratory  
P.O. Box 451  
Princeton, NJ 08543

Phone: 609-243-2245  
Fax: 609-243-2751  
e-mail: [pppl\\_info@pppl.gov](mailto:pppl_info@pppl.gov)  
Internet Address: <http://www.pppl.gov>